Enhanced Infrared Neural Stimulation using Localized Surface Plasmon Resonance of Gold Nanorods

Kyungsik Eom, Jinhyung Kim, Jong Min Choi, Taekyeong Kang, Jin Woo Chang, Kyung Min Byun, Sang Beom Jun,* and Sung June Kim**

A variety of external stimuli have been employed to modulate the activity of nerve cells by means of a local perturbation of extracellular environments.[1] To date, electrical stimulation of neurons has been mainly used because it is well-established in terms of precise quantification, easy controllability and high reliability. However, due to the limitations of invasiveness and poor spatial selectivity,[2] alternative techniques have been proposed such as ultrasound stimulation,[3] magnetic stimulation,[4] optical stimulation,[2] and optogenetic method.[5] Among them, the optical stimulation has been spotlighted in modulating a neural activity because light waves in visible and infrared bands can be delivered to the target area via artifact-free, damage-free and contact-free stimulation.[6,7] In particular, infrared neural stimulation (INS) is gaining an increasing attention owing to its advantages such as large penetration depth and high spatial selectivity.[8,9]

As an example, it was demonstrated that a pulsed, mid-infrared laser light could stimulate the neurons only in the direct optical path and be utilized to improve a cochlear implant system.[10,11] It is also interesting to note that successful INS approach is accompanied by temperature elevation in the vicinity of neurons. It implicates the local thermal heating at neuronal plasma membrane for the trigger of action potentials. While the underlying mechanism is not clarified yet, it has been hypothesized that the depolarization of neuron cell is associated with an activation of temperature-sensitive ion channels (e.g., TRPV channels) by the thermal heating of neurons and/or the change of the membrane conductance or capacitance.[6,12–14]

Recently, gold nanoparticles of various shapes including nanospheres, nanorods, and nanoshells have been frequently used to offer a light-induced functionality due to their unique optical property, called localized surface plasmons (LSPs).[15,16] Illumination at their resonant frequency leads to an efficient light absorption, where the absorbed energy is converted to heat.[17] Unlike propagating surface plasmons supported by a planar gold surface, nanoparticle plasmons induce the quantized electron oscillations confined to nanoscale volume, providing a means for manipulating light-matter interaction. Hence, plasmonically triggered local heat can activate the temperature-sensitive ion channels and cause an influx of calcium ions, therefore stimulating the neurons with a high spatial precision.

Intriguingly, it was reported that laser exposure combined with gold nanorods (GNRs) in neuronal cells can stimulate differentiation, particularly with regard to an increase in neurite outgrowth.[18] It appeared to be linked to transient heating arising from an excitation of LSP mode in GNRs, which can promote cell metabolic activity. While the results are noteworthy, use of a continuous wave mode and a long irradiation time has trouble with a potential tissue damage and imposes serious constraints on a repetitive neural excitation.

In this study, we intend to demonstrate an advanced optical stimulation strategy based on pulsed INS and plasmonic GNRs. Compared with previous approaches, we find that the suggested method is more advantageous in terms of neural responsivity, stimulation efficiency and spatial resolution, and in especial, can reduce the requisite radiant exposure level and alleviate the concern of tissue damage. It is therefore expected that we could open up new possibilities for applications to non-invasive investigations of diverse excitable tissues and treatments of neurological disorders.

K. Eom, Prof. S. J. Kim
Department of Electrical
and Computer Engineering
Seoul National University
Seoul 151–744, Republic of Korea
E-mail: kimsj@snu.ac.kr

J. Kim, Prof. J. W. Chang
Department of Neurosurgery
College of Medicine
Yonsei University
Seoul 120–752, Republic of Korea

J. M. Choi, Prof. K. M. Byun
Department of Biomedical Engineering
Kyung Hee University
Yongin 446–701, Republic of Korea
E-mail: kmbyun@khu.ac.kr

T. Kang, Prof. S. B. Jun
Department of Electronics Engineering
Ewha Womans University
Seoul 120–750, Republic of Korea
E-mail: juns@ewha.ac.kr

Prof. S. B. Jun
Department of Brain and Cognitive Sciences
Ewha Womans University
Seoul 120–750, Republic of Korea

DOI: 10.1002/smll.201400599

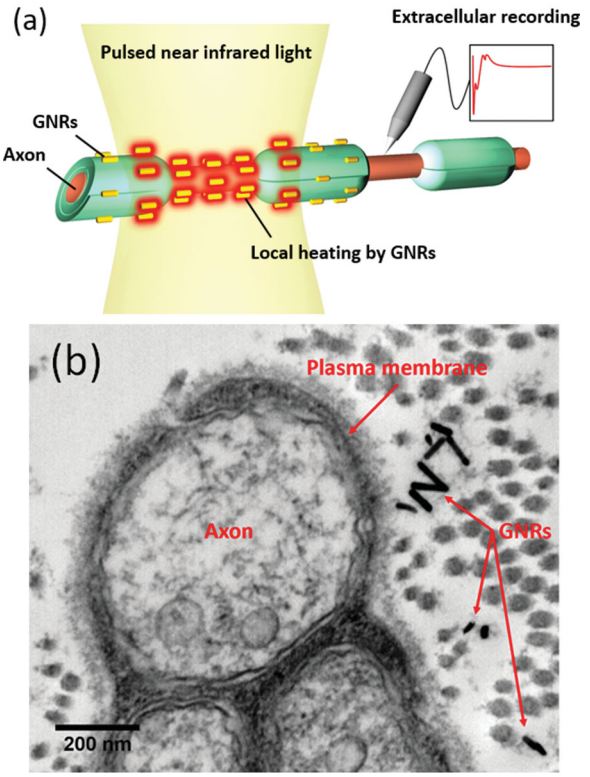

Figure 1. Concept of optical neural stimulation using localized heating of gold nanorods. a) Gold nanorods distributed in the vicinity of the plasma membrane of nerve tissues are designed to absorb a light energy at 980 nm wavelength. Pulsed infrared illumination photothermally heats the gold nanorods, causing a local temperature increase at the membrane of neural tissues. b) TEM image showing a cross-sectional view of rat sciatic nerve after injecting gold nanorods. Gold nanorods are located near the surface of the plasma membrane.

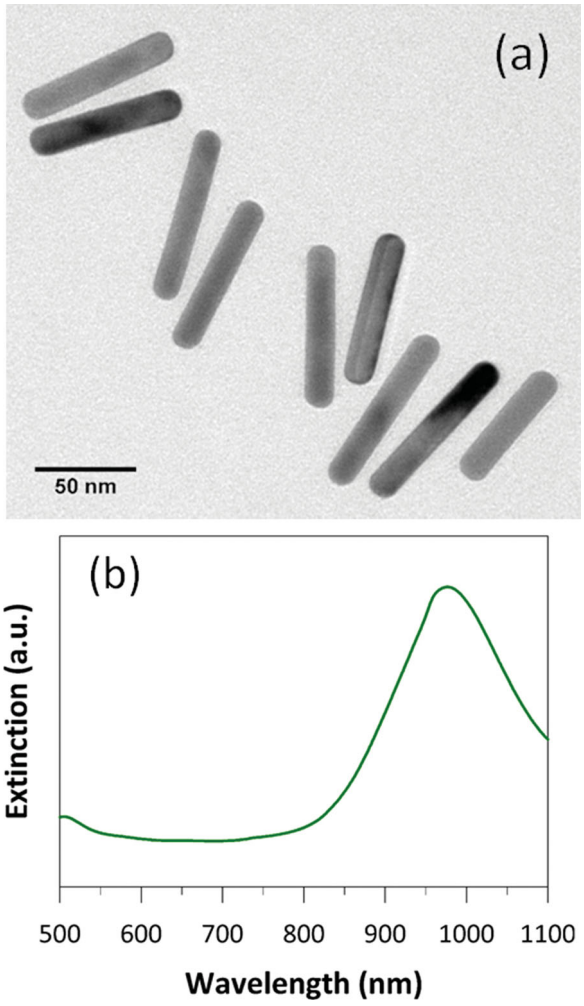

Figure 2. Experimental characterization of gold nanorods. a) TEM image of gold nanorods with a geometric dimensions of length = 80.4 nm and width = 15.3 nm. b) A graphs of extinction spectrum of gold nanorods showing a maximum absorption peak at $\lambda = 977$ nm.

Figure 1a illustrates the concept of experimental setup. Infrared light source is positioned at 50 mm away from the target neural tissue and the stimulation location is adjusted by red probing beam of 2-mm diameter. Real-time monitoring of compound nerve action potentials (CNAPs) in response to the optical stimulation is performed using electrical extracellular recording system.[9] In order to confirm the presence of GNRs near the plasma membrane, we examined a histological study using transmission electron microscopy (TEM) after injecting GNRs into nerve bundle. According to Figure 1b, GNRs are distributed in the vicinity of the plasma membrane of axons for local heating of the targeted nerves. Non-uniformity in size and shape of GNRs is attributable to a thin sectioning of the sample for TEM imaging. When GNRs are injected into a soft biological tissue, they are embedded with random orientations. As our tissue sectioning procedure produces a 5-nm thick thin slice, randomly oriented gold nanorods can be cut during the sample preparation.

TEM image in **Figure 2**a presents that the nanorod has average values in width of 15.3 nm and in length of 80.4 nm and its aspect ratio is thus 5.3. These length and width measurements are from particle size statistics of over 50 nanorods. The extinction spectra of the synthesized GNRs for in vivo experiments are shown in Figure 2b. The extinction maximum was observed at 977 nm, which is closed to the stimulation wavelength of $\lambda = 980$ nm. As the GNRs within the neural tissue can cause an efficient plasmonic absorption of a light energy at the resonance condition,[19] we hypothesized that neural tissue is activated at a considerably reduced laser intensity, while the INS without GNRs requires a high-level light energy.[20]

Prior to stimulating the neural tissues, in order to characterize the photothermal conversion efficacy of colloidal GNRs, heat generation by infrared irradiation was monitored using an infrared thermal camera. Following pulsed infrared irradiation using a 980 nm laser of 1 ms duration and 1 s interval, local temperature at the illumination point was rapidly elevated along with increasing the stimulation energy. When a 15 μL solution containing GNRs of a concentration of 3.4×10^{12}/mL was irradiated by the laser at 0.0324 J/pulse, temperature was increased by more than 6 °C within 1 min (Supporting Information, Figure S1). On the other hand, we could not find any notable change in temperature for 15 μL water solution without GNRs. These results imply that GNR plays an important role in producing a significant

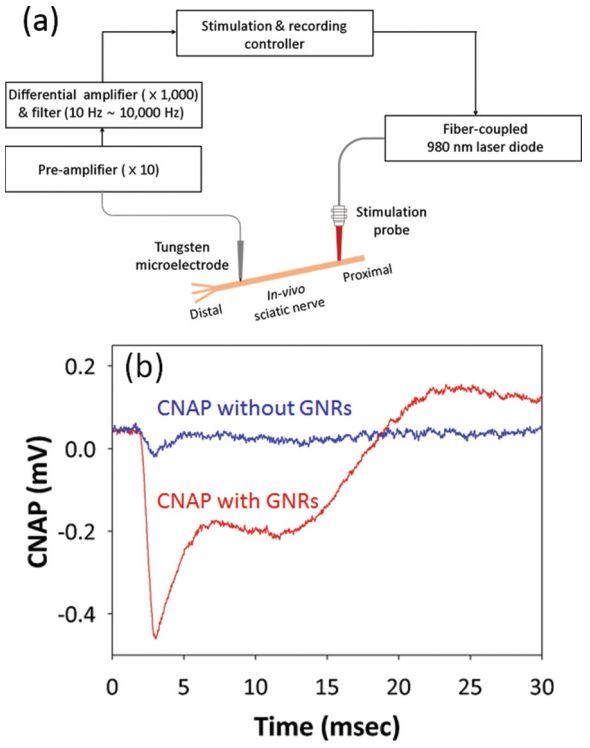

Figure 3. Compound nerve action potentials recorded from a rat sciatic nerve in vivo. a) An experimental setup for optical stimulation and electrical recording of in vivo rat sciatic nerve. b) CNAP curves recorded when a laser pulse with an exposure energy of 0.641 J/cm^2 was irradiated to the target nerves with and without gold nanorods.

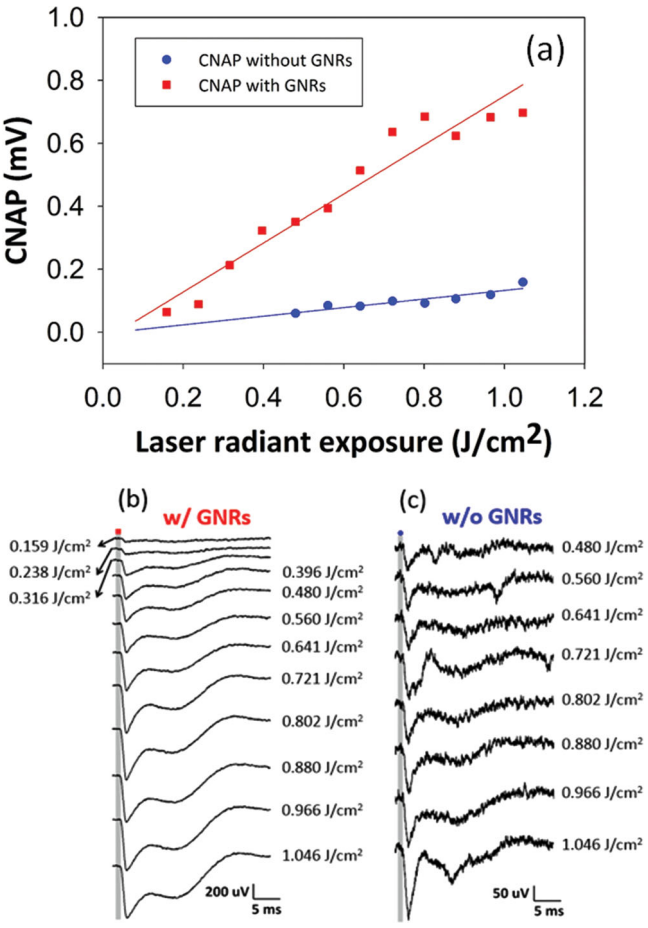

Figure 4. Compound nerve action potentials recorded while stimulating a rat sciatic nerve with an increasing laser intensity. a) Graphs of laser radiant exposure versus peak amplitude of the evoked CNAP during the stimulation. Neural stimulation with gold nanorods shows 5.7 times higher responsivity and three times lower stimulation thresholds than the one without gold nanorods. b) CNAPs recorded for 12 different laser powers when the sciatic nerves containing gold nanorods are stimulated. c) CNAPs recorded for 8 different laser powers when the sciatic nerves with no gold nanorods are stimulated (control).

temperature change in the vicinity of the plasma membrane of neural tissues and thereby triggers the action potentials.

Subsequently, to present that a pulsed infrared stimulation elicits a neuronal depolarization, we measured CNAPs from in vivo rat sciatic nerves using male Spraque-Dawley rats aged 10 weeks. All animals were treated in accordance with the animal research guidelines of Use Committee of the Institute of Laboratory Animal Resources at Seoul National University. The sciatic nerve with a length of ≈50 mm from the left thigh was exposed and the surrounding tissues were extracted before the stimulation. Fiber-coupled laser at λ = 980 nm illuminated the proximal part of the nerve bundle where a 1 µL of GNR solution was injected in advance using micro-injector at a rate of 23 nL/s while extracellular electrical recording was performed at the distal end (**Figure 3**a). During the experiments, optically evoked CNAPs were amplified, filtered and averaged sequentially. Figure 3b shows an exemplar of neural recording results upon the use of GNRs. While both INS strategies resulted in CNAPs under identical laser exposure of 0.641 J/cm^2, larger neural responses were produced in the presence of GNRs by more than 6 times. This clearly demonstrates that laser energy is delivered to the target tissue more effectively through its conversion to LSP modes excited by GNRs and the resultant local heating initiates more number of neurons to be activated. While the results are not shown here, the INS-induced CNAPs were found to disappear at the presence of voltage-gated Na^+ channel blocker, lidocaine, confirming that the CNAPs originate from neuronal activity.

Having found out the possibility that GNR-based INS elicits evoked potentials, we investigated its effectiveness on neural activation in two aspects: responsivity and threshold. **Figure 4**a shows the direct comparison of CNAPs with and without GNRs as a function of laser intensity. When a laser exposure is maintained at less than 1.0 J/cm^2 to avoid damaging the plasma membrane, an increase in stimulation power causes an activation of more number of neurons and leads to a corresponding amplitude increment of CNAP signals. Figure 4b,c shows the measured CNAP curves when rat sciatic nerves with and without GNRs are stimulated by a pulsed near infrared laser light in the range from 0.159 J/cm^2 to 1.046 J/cm^2. Of importance is that the linear regression data obtained from the case with GNR show a steeper slope by 5.7 times. It is likely that the enhanced responsivity is attributed to an effect of local heat generation which accelerates the depolarization of neuron cells inside the nerve bundles. In addition, for determining a stimulation threshold, we measured minimum laser intensity required to detect a

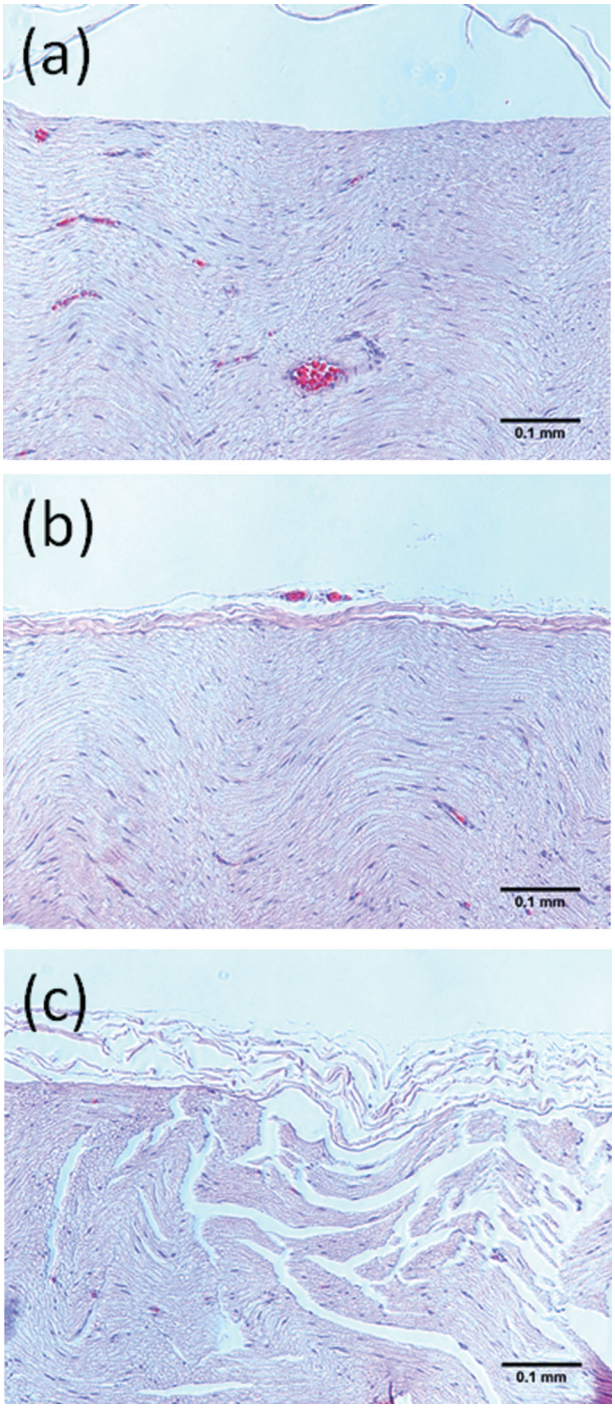

Figure 5. Histology (H&E stain) of nerve tissue upon laser exposure of various intensities. a) The sham specimen does not show any evidence of pathologic abnormality (negative control). b) The nerve irradiated at the stimulation energy of 0.956 J/cm^2 does not show any evidence of thermal damage. c) Significant histological changes in the nerve stimulated at the energy of 2.23 J/cm^2 were observed (positive control).

neural signal with an averaged magnitude of 60 μV. With an increasing laser power, stimulation thresholds were found to be 0.159 J/cm^2 for the INS with GNRs and 0.480 J/cm^2 for the one without GNRs. The latter is three times bigger than the former, which implies that the GNR-based INS is more advantageous in terms of efficiency and safety in nerve stimulation. Summarizing the results, due to a local temperature elevation by GNRs, we can invigorate temperature-sensitive ion channels, generating more neural activities and larger CNAP signals and therefore yielding an improvement in responsivity and stimulation threshold.

Finally, we performed the histological analysis of the sciatic nerve exposed to laser irradiation to assure our stimulation safety for the target tissues. Various radiant exposures in a wide power range were used to induce tissue damages for positive control. Twenty pulses with different radiant exposures from 0.32 J/cm^2 to 2.43 J/cm^2 were applied to the rat sciatic nerve embedded via paraffin. Serial 5 μm thick sections of the entire nerve were cut and stained with hematoxylin and eosin (H&E) to demonstrate pathological changes in the tissue. A sham procedure with no laser stimulation was also performed for negative control. **Figure 5**a exhibits the histological image of cross-sectional view of rat sciatic nerve for the negative control indicating no signs of damage. On the other hand, the histological analysis in Figure 5c for stimulation of 2.23 J/cm^2 presents a significant tissue damage, while stimulating with an exposure of 0.96 J/cm^2 causes no damage of nerve as shown in Figure 5b. Note that, in this study, we used the data obtained at an exposure level less than 1.0 J/cm^2 to guarantee a damage-free stimulation.

In summary, we successfully established the remote activation of neural tissues using photothermal effect by plasmonic GNRs. We demonstrated the advantages of our approach over conventional INS methods by increasing a neural responsivity and lowering a threshold level. Under the safe stimulation level to avoid a nerve damage, thermal activation of the plasma membrane in axon triggers action potentials of in vivo neural tissues. This approach can be adapted to stimulate diverse excitable tissues and moreover, be used to remotely manipulate other neural systems and treat neurological disorders.

Experimental Section

Nanoparticle Preparation and Characterization: Rod-shaped gold nanoparticles (C12–10–980, Nanopartz Inc, Loveland, CO, USA) with a concentration of 3.4 × 10^{13}/mL were prepared. The shape and size of gold nanorods were monitored via the 120 kV energy-filtering transmission electron microscope (Libra 120, Carl Zeiss, Germany). The extinction spectrum was measured using a wide-band spectrophotometer (UV-1800, Shimadzu, Japan).

Nanoparticle Injection and Visualization: Gold nanorods were prepared and injected to the sciatic nerve in vivo. Injection was conducted using microprocessor-controlled injection system (Nanoliter 2010, World Precision Instruments, Sarasota, FL, USA) which was mounted on a micromanipulator.[21] A 75 μm diameter, 30° beveled pulled glass capillary injection tip (SBB-75X-00, Sunlight Medical, Jacksonville, FL, USA) was coupled with the injection system. Gold nanorods were filled in the glass capillary tip via front filling. The tip was moved until it pierced the tissue. Once the penetration was achieved, the nanorod was injected at the rate of 23 nL/s. The distribution of gold nanorods inside the nerve bundle was visualized as follows. Sciatic nerve bundle was excised and the

NANO MICRO small

specimen was fixed via Karnovsky's fixation (primary fixation). Washing out the Karnovsky's solution by 0.05 M sodium cacodylate buffer was, then, followed. Lipid fixation was conducted (post fixation, 2% osmium tetroxide and 0.1 M cacodylate buffer). After washing the sample, an en-block staining was performed. The samples were dehydrated by soaking into the ethanol solution. Infiltration by spurr's resin was performed after transiting the environment as the resin friendly by propylene oxide. The polymerized specimen block was sectioned with a 5 nm thickness via ultramicrotome (MTX, RMC, USA). The sample was reviewed via the 80 kV TEM (JEM1010, JEOL, Japan).

Optical Stimulation and Electrical Recording System: Fiber-coupled laser diode (Pearl P14 Series, nLIGHT, Vancouver, WA, USA) was used to stimulate the rat sciatic nerve. At the end of the fiber, collimator and focusing lens were installed. Optically evoked responses were recorded via electrical recording system. From the preamplifier (×10), optically evoked signals were pre-amplified and were fed into the differential AC amplifier (Microelectrode AC Amplifier Model 1800, AM systems, Carlsborg, WA, USA) whose gain was set as 1000 and band-pass filter was ranged from 10 Hz to 10 kHz. Amplified electrical signals were recorded with a data acquisition system (PXI-4462, National Instruments, Austin, TX, USA). Data recording were pre-triggered 1.6 ms prior to the optical stimulation pulse and the signal were monitored while 15 signals were averaged simultaneously.

Bulk Solution Heating: A 15 µL solution containing gold nanorods with a concentration of 3.4×10^{13}/mL was filled in the micropipette tip which was mounted with a pipette. Pulsed infrared light at a duration of 1 ms and an interval of 1 s was provided by the fiber-coupled laser diode and was focused on the center of the solution. The solution was exposed to laser beam repeatedly with increasing its intensity (0.0106 J/pulse, 0.0215 J/pulse, 0.0324 J/pulse, 0.0433 J/pulse, and 0.0532 J/pulse). The temperature of aqueous dispersion was monitored via infrared thermal camera (T400, FLIR, USA).

Animal Preparation and Identification of Laser Mediated Tissue Damage: Spraque-Dawley rat (≈350 g) was anesthetized with intraperitoneal injection of urethane (1.5 g/kg). To access the sciatic nerve, an incision was made from the biceps femoris muscle to the gluteus muscle. The muscle covering the nerve was carefully removed to expose the nerve surface while continually moistened with saline buffer. For identification of laser mediated tissue damage, the nerve was excised and immediately subjected to laser irradiation. The nerve was, then, placed in 4% paraformaldehyde solution and sent for the paraffin embedding. The tissue block was sectioned sagittally with 4 µm thickness and placed on the glass slide. The tissues were stained with hematoxylin and eosin (H&E).[22] All the sections were reviewed using a photomicroscope (Axiophot, Carl Zeiss, Germany).

Supporting Information

Supporting Information is available from the Wiley Online Library or from the author.

Acknowledgements

This work was supported by the Brain Korea 21 Plus Project, the Department of Electrical and Computer Engineering, Seoul National University in 2014 and by the Pioneer Research Center Program through the National Research Foundation of Korea funded by the Ministry of Education, Science and Technology (NRF-2009–0082961 and Global Frontier Project (CISS-2013072261)). This work was also supported by the National Research Foundation of Korea (NRF) grants funded by the Korea government (MEST) (2011–0029485, 2011–0014529, 2012–0003809, NSF-2013R1A1A1A05011990, and NSF-2014R1A1A1A05003770), the Public Welfare & Safety research program of the Ministry of Education, Science and Technology (NRF-2010–0020851) and the Technology Innovation Program (10033657) of the Ministry of Knowledge Economy (MKE).

[1] K. Franze, J. Guck, *Rep. Prog. Phys.* **2010**, *73*, 094601.
[2] J. Wells, C. Kao, E. D. Jansen, P. Konrad, A. Mahadevan-Jansen, *J. Biomed. Opt.* **2005**, *10*, 064003.
[3] Y. Hu, W. Zhong, J. M. F. Wan, A. C. H. Yu, *Ultrasound Med Biol.* **2013**, *39*, 915.
[4] M. Kobayashi, A. Pascual-Leone, *Lancet Neurol.* **2003**, *2*, 145.
[5] E. S. Boyden, F. Zhang, E. Bamberg, G. Nagel, K. Deisseroth, *Nat. Neurosci.* **2005**, *8*, 1263.
[6] M. G. Shapiro, K. Homma, S. Villarreal, C.-P. Richter, F. Bezanilla, *Nat. Commun.* **2012**, *3*, 736.
[7] A. R. Duke, M. W. Jenkins, H. Lu, J. M. McManus, H. J. Chiel, E. D. Jansen, *Sci. Rep.* **2013**, *3*, 2600.
[8] J. Wells, C. Kao, K. Mariappan, J. Albea, E. D. Jansen, P. Konrad, A. Mahadevan-Jansen, *Opt. Lett.* **2005**, *30*, 504.
[9] J. Wells, P. Konrad, C. Kao, E. D. Jansen, A. Mahadevan-Jansen, *J. Neurosci. Methods* **2007**, *163*, 326.
[10] A. D. Izzo, E. Suh, J. Pathria, J. T. Walsh, D. S. Whitlon, C. P. Richter, *J. Biomed. Opt.* **2007**, *12*, 021008.
[11] C. P. Richter, R. Bayon, A. D. Izzo, M. Otting, E. Suh, S. Goyal, J. Hotaling, J. T. Walsh Jr., *Hear. Res.* **2008**, *242*, 42.
[12] C. P. Richter, A. I. Matic, J. D. Wells, E. D. Jansen, J. T. Walsh, *Laser Photonics Rev.* **2011**, *5*, 68.
[13] J. Wells, C. Kao, P. Konrad, T. Milner, J. Kim, A. Mahadevan-Jansen, E. D. Jansen, *Biophys. J.* **2007**, *93*, 2567.
[14] E. J. Katz, I. K. Ilev, V. Krauthamer, D. H. Kim, D. Weinreich, *Neuro-Report* **2010**, *21*, 662.
[15] E. Hutter, J. H. Fendler, *Adv. Mater.* **2004**, *16*, 1685.
[16] M. E. Stewart, C. R. Anderton, L. B. Thompson, J. Maria, S. K. Gray, J. A. Rogers, R. G. Nuzzo, *Chem. Rev.* **2008**, *108*, 494.
[17] G. Baffou, R. Quidant, *Laser Photonics Rev.* **2013**, *7*, 171.
[18] C. Paviolo, J. W. Haycock, J. Yong, A. Yu, P. R. Stoddart, S. L. McArthur, *Biotechnol. Bioeng.* **2013**, *110*, 2277.
[19] C. F. Bohren, *Am. J. Phys.* **1983**, *51*, 323.
[20] L. R. Hirsch, R. J. Stafford, J. A. Bankson, S. R. Sershen, R. E. Price, J. D. Hazle, N. J. Halas, J. L. West, Proc. Second Joint EMBS/BMES Conf., Houston, TX, USA **2002**.
[21] G. Fischer, S. Kostic, H. Nakai, F. Park, D. Sapunar, H. Yu, Q. Hogan, *J. Neurosci. Methods* **2011**, *199*, 43.
[22] J. D. Wells, S. Thomsen, P. Whitaker, E. D. Jansen, C. C. Kao, P. E. Konrad, A. Mahadevan-Jansen, *Lasers Surg. Med.* **2007**, *39*, 513.

Received: March 6, 2014
Revised: May 6, 2014
Published online: June 27, 2014

